Hindawi
Wireless Communications and Mobile Computing
Volume 2022, Article ID 3940132, 11 pages
https://doi.org/10.1155/2022/3940132

Research Article

Optimal Time Allocation for Energy Harvesting Cognitive Radio Networks with Multichannel Spectrum Sensing

Xiaoying Liu, Ming Xia, Ping Hu, Kechen Zheng, and Shubin Zhang

School of Computer Science and Technology, Zhejiang University of Technology, China

Correspondence should be addressed to Kechen Zheng; kechenzheng@zjut.edu.cn

Received 29 June 2022; Accepted 3 August 2022; Published 21 August 2022

Academic Editor: Lei Liu

From the perspective of time domain and frequency domain, we investigate the energy harvesting cognitive radio networks (EH-CRNs) with multichannel, where the secondary transmitter (ST) opportunistically accesses the licensed subchannels to transmit packets by consuming the harvested energy. To explore the spectrum holes and improve the lifetime of the EH-CRNs, the ST scavenges energy from the radio-frequency (RF) signal in the wide band during the energy harvesting (EH) phase and exploits the harvested energy for sequential sensing and packet transmission during the rest of the time slot. Under the energy constraint, the secondary throughput is improved by optimizing the time allocation among the EH phase, sensing phase, and transmission phase. We formulate the secondary throughput with respect to the durations of the three phases, prove the existence of the optimal time allocation, and discuss the secondary throughput in three cases of the EH-CRNs. Finally, numerical results validate the theoretical results about the secondary throughput and explore the impacts of key system parameters.

1. Introduction

With the fast development of Internet of Things (IoT), a huge amount of data is generated everyday [1–3], and the increasing pressure on the spectrum deficit and energy consumption problems has attracted a large amount of attention [4, 5]. Researchers are exploring novel access schemes for the wireless communications, such as multiple-input-multiple-output (MIMO) [6] and cognitive radio (CR). To improve spectral efficiency under the fixed spectrum assignment policy, CR is proposed as a promising technology by allowing secondary users (SUs) to opportunistically access the spectrum licensed to primary users (PUs) [7, 8]. To improve the lifetime of IoT devices and mitigate the energy deficit problem, energy harvesting (EH) is proposed as an important technology by scavenging energy from the renewable energy sources in the environment, such as solar, wind, and radio frequency (RF) signals [9]. Comparing with the other energy sources, the RF signal holds a more promising future due to its predictable, stable nature, and low cost [10]. Incorporating the CR and EH technologies raises the concern about EH-CR network (EH-CRN), where EH provides more energy supply for SUs to sense the state of the licensed spectrum [11].

In the CRNs, there are generally multiple licensed channels for SUs to opportunistically access without affecting the primary transmission. By providing the access to a wide range of spectrum with less complexity and computational cost for the SUs, the network performance could be significantly enhanced [12]. Hence, multichannel is an important perspective for the CRNs to achieve better performance as well as protect the primary transmission [13–16]. By proposing sequential spectrum sensing algorithms, Kim and Giannakis [13] reduced the required sample size to meet the specified reliability target and evaluated the SUs' collision constraints to protect primary transmission. Kang et al. [14] investigated the dynamic spectrum access in the multichannel CRN by formulating the channel information market as a two-stage Stackelberg game. Cheng et al. [15] developed a full-duplex based framework to improve resource utilization in the multichannel CR ad hoc networks. To improve the number of successful transmissions without interrupting primary transmission in the multichannel wireless networks, Li et al. [16] addressed the challenge of

unknown system dynamics and computational expenses by the deep Q-network.

The network performances in [12–16] may degrade severely when the issue of energy supply for the SUs is taken into account. Therefore, the strategy and details of multichannel spectrum sensing need to be delicately designed to mitigate the energy deficit problem. To be specific, Celik and Kamal [17] proposed energy efficient cooperative spectrum sensing (CSS) policies for multichannel green CRNs, with the objectives to minimize the total energy consumption and maximize the total throughput. To minimize the energy consumption of sensing subject to the requirements of sensing accuracy, Ejaz and Ibnkahla [18] formulated an optimization problem to determine a minimum number of channels to be sensed in the multiband approach. To minimize the sensing time and maximize the amount of the harvested energy, Alsharoa et al. [19] jointly optimized the number of sensing samples and sensing threshold in the CRNs with multiband. Thanh et al. [20] maximized the security of the multichannel cognitive system, where the limited-battery SU is powered by a solar energy harvester. With the aim to reduce energy consumption and evaluate network lifetime, Bagheri and Ebrahimzadeh [21] presented a probabilistic approach in the cognitive sensor network with multichannel CSS.

As aforementioned, some previous works have pointed out the advantage of CSS by multiple SUs [12, 13, 17, 18, 21] and minimized the energy consumption to extend the network lifetime [12, 17, 18, 21]. However, as far as we know, only a few works have incorporated the EH functionality in the SUs, such as the RF EH in [19] and the solar EH in [20]. According to the advantages of RF EH [10], the fact that more energy consumption would be consumed by CSS due to multiple SUs participating in sensing one PU [22], it is of great significance to explore the tradeoff among the duration of EH, the sensing performance, and the sensed available channels in the EH-CRNs with multichannel.

In this paper, we investigate the issue of time allocation for RF-powered EH-CRNs, where the secondary transmitter (ST) first harvests energy from the RF signals in the multichannel, determines the number of licensed subchannels to sense, and then exploits the inactive channels to transmit packets to the SR by consuming the harvested energy. What should be pointed out is that we have investigated the multichannel spectrum sensing performed by the multiantenna ST with EH functionality in [23], where we coordinate the time scheduling and energy management to improve the spectrum utilization efficiency. Therefore, the tradeoff between the duration of packet transmission and the consumed energy for transmission has not been well addressed in [23]. Besides, Alsharoa et al. [19] adopted a time switching protocol, where SUs switch over time between sensing and EH, while the time tradeoff among the EH phase, sensing phase, and transmission phase has not been studied. This paper differs from previous works in the following two aspects. First, unlike most of the aforementioned studies, we consider the ST exploits the sensed available channels for packet transmission, as the access to a wide range of spectrum in [12]. Second, the duration of EH phase, the number of sensed subchannels in sensing phase, and the duration of transmission phase are considered as variables for the time tradeoff, where the sensing time of one subchannel by the ST is predesigned to ensure the sensing performance. In the time tradeoff, the ST follows the energy constraint that the energy consumption of sequential sensing and packet transmission could not exceed the amount of the harvested energy.

Motivated by the above discussion, we summarize the main contributions of this paper as follows.

(i) To maximize the secondary throughput with the collision and energy constraints, we investigate the optimal time allocation among the EH phase, sensing phase, and transmission phase in the EH-CRNs, where the ST is exclusively powered by RF multichannel EH and performs sequential sensing and packet transmission

(ii) By proving the concavity of the expected secondary throughput with respect to the duration of three phases through monotonicity analysis, we prove the existence of the optimal time allocation and separately discuss the solutions in three cases of the EH-CRN. The optimal number of sensed channels only depends on the EH power of the ST, the sensing time of one subchannel, and the energy consumed for sensing one subchannel

(iii) Numerical results are provided to validate the existence of the maximum secondary throughput with respect to the optimal time allocation, which is in accordance with the derived theoretical result. Moreover, numerical results reveal the impacts of system parameters, i.e., the EH power of the ST

The rest of this paper is organized as follows. In Section 2, we introduce the system model and key notations. In Section 3, we formulate the secondary throughput and the collision probability. In Section 4, we optimize the time tradeoff among the EH phase, sensing phase, and transmission phase. In Section 5, we analyze the time tradeoff in the three cases of the EH-CRNs. Discussions and numerical results are provided in Section 6. Finally, conclusions are drawn in Section 7.

2. System Model

The EH-CRN is introduced from three aspects: network model, spectrum sensing model, and transmission model. The first aspect introduces the network topology, the PUs, and SUs. The rest aspects specify the process that the ST opportunistically accesses the multichannel spectrum by consuming the harvested energy. To facilitate reading, we summarize key notations adopted throughout the paper in Table 1.

2.1. Network Model. We consider a CRN consisting of M primary pairs and one secondary pair and divide a given wide frequency band into M subchannels of equal

Table 1: Key notations.

Symbol	Definition
M	Number of subchannels in the EH-CRN
B	The bandwidth of each subchannel
P_k	Transmit power of the PT in the kth subchannel
P_h	EH power of the ST
p_a	Probability that each subchannel is active
e_h	Energy harvested in one time slot
e_s	Energy consumed for sensing one subchannel
t_h	Duration of EH phase
t_s	Sensing time of one subchannel
t_t	Duration of transmission phase
x	Number of sensed subchannels in sensing phase
x_s	Number of correctly sensed inactive subchannels
h_k	Channel gain of the kth subchannel
h	Channel gain from the ST to the SR
$p_{d,k}$	Probability of detection for subchannel k
$p_{f,k}$	Probability of false alarm for subchannel k
$p_{c,x}$	Collision probability

bandwidth B, which are assigned to the M primary pairs, respectively. Each primary pair has license to access one unique subchannel, and the states of the subchannels are considered to be independent of each other. The arrival of primary packets follows a time-homogeneous random process, where the subchannels licensed to the primary network switch between the active state and the inactive state. Let p_a denote the probability that each subchannel is active, where $0 < p_a < 1$ holds.

As illustrated by [24], the SUs can synchronize with PUs when they have perfect knowledge of PUs' communication mechanism. Hence, we consider that the PUs and SUs adopt a synchronous slotted protocol with unit length, which consists of EH phase, sensing phase, and transmission phase, as illustrated in Figure 1. The secondary pair consists of an EH ST and a secondary receiver (SR). During the EH phase, the ST harvests energy from the RF signal in the wide band, which could be implemented by the multichannel EH scheme in Figure 3 of [19]. Then, we estimate the EH power of the ST, denoted by P_h, as

$$P_h = \eta p_a \sum_{k=1}^{M} P_k h_k, \tag{1}$$

where P_k denotes the transmit power of the primary transmitter (PT) in the kth subchannel, h_k denotes the channel gain of the kth subchannel, and η denotes the efficiency of the energy harvester in the ST, where $1 > \eta > 0$ holds. In the synchronous slotted protocol with unit length, t_h denotes the duration of EH phase. Thus, the amount of the energy harvested by the ST in one time slot, denoted by e_h, can be obtained as

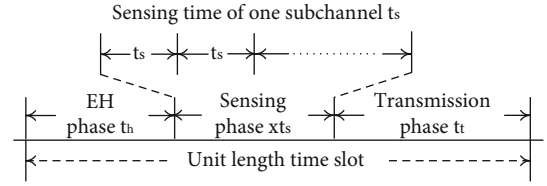

Figure 1: Slot structure.

$$e_h = t_h P_h. \tag{2}$$

Then, the ST consumes the harvested energy to perform spectrum sensing and packet transmission in the rest of the time slot. Therefore, as shown in Figure 1, the EH phase precedes the sensing phase and transmission phase in the synchronous slotted protocol.

2.2. Spectrum Sensing Model. In order to constrain the excessive interference from the ST to the PR, it is necessary for the ST to perform spectrum sensing in the EH-CRN. Due to the advantages of adequate performance, relatively simple practical realization [25], and low computational complexity [26], we employ the popular energy detection method for spectrum sensing. A binary hypothesis test could be built for the subchannel k ($1 \le k \le M$) by the ST as follows:

$$\begin{cases} \mathcal{H}_{0,k}: & y_k(m) = n_k(m), \\ \mathcal{H}_{1,k}: & y_k(m) = s_k(m) + n_k(m), \end{cases} \tag{3}$$

where $\mathcal{H}_{0,k}$ and $\mathcal{H}_{1,k}$ represent the inactive spectrum state and active spectrum state of the subchannel k, respectively. In (3), $y_k(m)$ represents the m-th sample of the subchannel k at the ST's energy detector, and $s_k(m)$ and $n_k(m)$ represent the primary RF signal and the noise of the subchannel k at the ST, respectively. As pointed out in [27], both the primary signal and noise can be modeled as independent circularly symmetric complex Gaussian (CSCG) random processes with variances $\sigma_{p,k}^2$ and $\sigma_{n,k}^2$, respectively. In general, we approximate $\sigma_{n,k}^2 = \sigma_n^2$. In such a case, under hypothesis $\mathcal{H}_{1,k}$, the probability of detection for subchannel k, denoted by $p_{d,k}$, can be expressed as follows [27].

$$p_{d,k} = \mathbb{P}\left\{r_k = 1 \middle| \mathcal{H}_{1,k}\right\} = \mathcal{Q}\left(\sqrt{\frac{f_s t_s}{2\gamma_k + 1}}\left(\frac{\varepsilon}{\sigma_n^2} - \gamma_k - 1\right)\right), \tag{4}$$

where $r_k \in \{0(\text{inactive}), 1(\text{active})\}$ represents the sensing result of subchannel k, f_s denotes the sampling frequency, and t_s denotes the duration of spectrum sensing for

subchannel k. $p_{d,k}$ represents the probability that the ST determines the channel k as active when the channel k is actually active. In (4), ε represents the detection threshold for the energy detector, and $\gamma_k = \sigma_{p,k}^2/\sigma_n^2$ denotes the signal-to-noise ratio (SNR) of the primary RF signal in subchannel k. $\mathcal{Q}(\cdot)$ is the complementary distribution function of the standard Gaussian [27] as

$$\mathcal{Q}(x) = \frac{1}{\sqrt{2\pi}} \int_x^{\infty} \exp\left(-\frac{y^2}{2}\right) dy. \tag{5}$$

Under hypothesis $\mathcal{H}_0$, the probability of false alarm for subchannel k, denoted by $p_{f,k}$, can be expressed as follows [27].

$$p_{f,k} = \mathbb{P}(r_k = 1 \mid \mathcal{H}_{0,k}) = \mathcal{Q}\left(\sqrt{f_s t_s}\left(\frac{\varepsilon}{\sigma_n^2} - 1\right)\right). \tag{6}$$

$p_{f,k}$ represents the probability that the ST determines the channel k as active when the channel k is actually inactive. In order to ensure a reasonable spectrum sensing performance by energy detection, we consider the values of the sensing time t_s, sampling frequency f_s, and detection threshold ε in the ST's energy detector are appropriately predesigned such that the employed energy detection has more than a half probability to obtain the correct result, i.e., $0.5 < p_{d,k} \le 1$ and $0 \le p_{f,k} < 0.5$, which is a reasonable consideration about sensing performance as that in [28, 29]. If without this consideration, the probability of correctly determining the spectrum state would be less than a half, and it is meaningless for the ST to perform spectrum sensing with such low accuracy. Then $p_{f,k}$ in (6) for subchannel k could be simplified as p_f with the same parameters t_s, f_s, and ε.

In addition, the value of the sensing time t_s for the M subchannels is considered as the same, which is a reasonable consideration for the subchannels with equal bandwidth and close center frequencies. Let e_s denote the amount of the energy consumed by the ST for sensing each subchannel during the sensing phase. When the ST senses x subchannels in a sequential manner, the duration of the sensing phase is xt_s, and the ST consumes xe_s amount of energy in the sensing phase, where x is an integer in the value interval $[0, M]$.

2.3. Transmission Model. In the transmission phase, the ST consumes the residual energy to transmit packets to the SR. In order to maximize the myopic secondary throughput of the time slot, as the proof and discussion of Lemma 1 [9], the ST should fully consume the residual energy to perform packet transmission with constant transmission power during the transmission phase. The myopic optimization concentrates solely on the immediate throughput reward, neglecting the impact of current operation on the future throughput reward [30]. Existing works have shown that myopic policy is optimal or at least close in performance to the optimal policy, while it has a simple structure and reduces the computational complexity [31]. Based on the Shannon's Formula [32], the transmission rate of the secondary pair, denoted by C_s, could be modeled as

$$C_s = x_s B \log\left(1 + \frac{(t_h P_h - xe_s)h}{t_t \sigma_n^2}\right), \tag{7}$$

where x_s denotes the number of subchannels that the ST correctly detects as inactive, $x_s B$ represents the detected inactive bandwidth for packet transmission, $(t_h P_h - xe_s)$ represents the nonnegative residual energy for packet transmission, h denotes the gain of the channel from the ST to the SR, t_t denotes the duration of transmission phase, and σ_n^2 represents the noise power for the secondary packet transmission. If $t_h P_h - xe_s \le 0$, the ST does not have energy for packet transmission, and $C_s = 0$ holds. Considering the synchronous slotted protocol with unit length, we have

$$t_h + xt_s + t_t = 1. \tag{8}$$

3. Performance Analysis of the EH-CRN

In this section, we first present four possible scenarios of spectrum sensing for each subchannel. Then, we formulate the expected secondary throughput and the probability of collision with the primary transmission.

3.1. Sensing Results. By employing an energy detection method in Section 2.2 for spectrum sensing, we have four possible scenarios for the sensing result of each subchannel. We take subchannel k as an example as follows.

(i) The ST correctly decides that subchannel k is inactive with probability $(1 - p_a)(1 - p_f)$. The subchannel k could be efficiently accessed by the ST to transmit packets to the SR in the transmission phase

(ii) The ST incorrectly decides that subchannel k is active with probability $(1 - p_a)p_f$. The subchannel k is inactive and will not be accessed by the ST in the transmission phase

(iii) The ST correctly decides that subchannel k is active with probability $p_a p_{d,k}$. The subchannel k is active and will not be accessed by the ST in the transmission phase

(iv) The ST incorrectly decides that subchannel k is inactive with probability $p_a(1 - p_{d,k})$. The subchannel k is active and will be accessed by the ST in the transmission phase, which results in a collision with the primary transmission

Based on the aforementioned four scenarios, we infer that the first case corresponds to the successful secondary transmission through subchannel k, which is adopted to formulate the expected secondary throughput in Section 3.2. We also infer that the fourth case corresponds to the collision between the primary transmission and secondary transmission in subchannel k and is adopted to formulate the probability of collision in Section 3.3.

3.2. Secondary Throughput. In this subsection, we formulate and analyze the expected throughput of the secondary pair,

denoted by $\lambda(t_h, x, t_t)$. The variables in $\lambda(t_h, x, t_t)$ include the duration of the EH phase t_h, the number of subchannels sensed by the ST x, and the duration of the transmission phase t_t.

Lemma 1. *The expected throughput of the secondary pair is expressed as*

$$\lambda(t_h, x, t_t) = x(1-p_a)\left(1-p_f\right)Bt_t \log\left(1+\frac{(t_hP_h - xe_s)h}{t_t\sigma_n^2}\right). \tag{9}$$

Proof. As presented in the first case of Section 3.1, since the states of the subchannels are considered to be independent of each other, we obtain the probability that i-out-of-x subchannels are inactive as

$$\binom{x}{i}(p_a)^{x-i}(1-p_a)^i, \tag{10}$$

where $x \geq i \geq 0$ holds. Among the i inactive subchannels, only j-out-of-i subchannels are correctly detected by the ST and could be used by the ST in the transmission phase, where $i \geq j \geq 0$ holds. We obtain the probability that j-out-of-i inactive subchannels are correctly decided as inactive as

$$\binom{x}{j}\left(p_f\right)^{x-j}\left(1-p_f\right)^j. \tag{11}$$

Based on (7), (10), (11), and the value interval of x in Section 2.2, the expected secondary throughput $\lambda(t_h, x, t_t)$ could be formulated as

$$\begin{aligned}\lambda(t_h, x, t_t) = \sum_{i=0}^{x}\Bigg\{&\binom{x}{i}(p_a)^{x-i}(1-p_a)^i \\ &\times\Bigg\{\sum_{j=0}^{i}\binom{i}{j}\left(p_f\right)^{x-j}\left(1-p_f\right)^j jBt_t \log \\ &\cdot\left(1+\frac{(t_hP_h - xe_s)h}{t_t\sigma_n^2}\right)\Bigg\}\Bigg\}.\end{aligned} \tag{12}$$

We observe that $Bt_t \log(1+(t_hP_h - xe_s)h/t_t\sigma_n^2)$ in (12) is independent of i and j. Then, we have

$$\begin{aligned}&\sum_{j=0}^{i}\binom{i}{j}\left(p_f\right)^{x-j}\left(1-p_f\right)^j j \overset{(a)}{=} \sum_{j=1}^{i}\binom{i}{j}\left(p_f\right)^{x-j}\left(1-p_f\right)^j \\ &\cdot j \overset{(b)}{=} \sum_{j=1}^{i}\binom{i-1}{j-1}\left(p_f\right)^{x-j}\left(1-p_f\right)^j i \overset{(c)}{=} \sum_{j'=0}^{i-1} i - \binom{i-1}{j'} \\ &\cdot\left(p_f\right)^{x-j'-1}\left(1-p_f\right)^{j'} i\left(1-p_f\right) \overset{(d)}{=} i\left(1-p_f\right).\end{aligned} \tag{13}$$

(a) in (13) holds due to the item with $j=0$ in the summation is equal to zero, (b) in (13) holds due to the sampling formula (20.1.1.4) in [33], (c) in (13) holds due to the $j' = j-1$, and (d) in (12) holds due to the characteristic of binomial distribution. Similarly, by using the simplification in (13), we have

$$\sum_{i=0}^{x}\binom{x}{i}(p_a)^{x-i}(1-p_a)^i i\left(1-p_f\right) = x(1-p_a)\left(1-p_f\right). \tag{14}$$

Based on (13) and (14), we simplify $\lambda(t_h, x, t_t)$ in (12) as (9). This completes the proof. □

The main focus of this paper is to maximize $\lambda(t_h, x, t_t)$ in (9) by optimizing the time tradeoff among the three phases in the slotted protocol, which will be presented in Section 4.

3.3. Collision Probability. In this subsection, we formulate and analyze the probability of collision in the EH-CRN, denoted by $p_{c,x}$. As shown in (7), if at least one of the x_s subchannels is incorrectly decided, the secondary transmission fails due to the completeness of secondary packets.

As presented in the fourth case of Section 3.1, we obtain the probability that i-out-of-x subchannels are inactive as (10). Then, the probability that all of the $(x-i)$ active subchannels are correctly decided could be represented as

$$\binom{x}{i}(p_a)^{x-i}(1-p_a)^i\prod_{l=1}^{x-i}p_{d,s_l}. \tag{15}$$

In (15), for $l \in [1, x-i]$, s_l is integers, and $1 \leq s_1 < s_2 < \cdots < s_{x-i} \leq M$ holds without loss of generality. (14) indicates that the detection probability of each subchannel could be chosen at most once in the multiplication. Based on (15), the probability of collision in the EH-CRN could be represented as

$$p_{c,x} = \sum_{i=0}^{x}\left\{\binom{x}{i}(p_a)^{x-i}(1-p_a)^i\left(1-\prod_{l=1}^{x-i}p_{d,s_l}\right)\right\}. \tag{16}$$

Then, we present the following lemma to analyze $p_{c,x}$.

Lemma 2. *The probability of collision $p_{c,x}$ is an increasing function of x.*

Proof. First, $p_{c,x}$ in (16) indicates that the probability that at least one of the active subchannels among the chosen x subchannels is incorrectly sensed. The complementary event is that all the active subchannels among the chosen x subchannels are correctly sensed. With imperfect sensing in the EH-CRN, it is easy to infer that the probability that all the active subchannels among the chosen $x+1$ subchannels are correctly sensed is smaller than the probability of the x subchannels case. To be specific, the event that all the active subchannels among the chosen x subchannels are correctly

sensed consists of the event that all the active subchannels among the chosen $x+1$ subchannels are correctly sensed and the event that one of the chosen $x+1$ subchannels is incorrectly sensed. Based on the characteristic of complementary event, this completes the proof. □

With a predesigned value of the maximum permissible collision probability, which is determined by the network designer and independent of other variables [7, 27] in the EH-CRN, we obtain an upper bound of x based on the monotonicity of $p_{c,x}$ in Lemma 2. This predesigned value of collision probability could be viewed as the protection of primary transmission against collisions to a certain extent.

4. Throughput Optimization

In this section, we optimize the time tradeoff among the EH phase, sensing phase, and transmission phase, in order to obtain the maximum of $\lambda(t_h, x, t_t)$. The collision constraint, i.e., the predesigned value of collision probability that the secondary transmission could not exceed, will be incorporated in the discussion about the maximum of $\lambda(t_h, x, t_t)$. We formulate the throughput optimization problem as

$$\max \lambda(t_h, x, t_t), \tag{17}$$

$$\text{s.t.} C1 : 1 > t_h > 0, \tag{18}$$

$$C2 : x > 0, \tag{19}$$

$$C3 : 1 > t_t > 0, \tag{20}$$

$$C4 : t_h + xt_s + t_t = 1, \tag{21}$$

where $C1 - C3$ represent the value intervals of the duration of each phase. Based on the following monotonicity analysis, we summary the theoretical results of the optimal time allocation for the throughput optimization problem as follows.

Theorem 3. *Under the constraints (18)-(21), the optimal time allocation, i.e., the optimal values of x and t_t, that maximizes the secondary throughput, if ever exists, should satisfy (33) and (34).*

Proof. Though x is defined as an integer in Section 2.2, the following analysis of the continuous function $\lambda(t_h, x, t_t)$, which regards x as a continuous variable, applies to the throughput analysis with integer x. Based on $C4$ in (21), we express t_h as a function of t_t and x. By bringing this function in $\lambda(t_h, x, t_t)$ of (16), we have

$$\lambda(t_h, x, t_t) = x(1-p_a)\left(1-p_f\right)Bt_t \times \log\left(1 + \frac{((1-t_t-xt_s)P_h - xe_s)h}{t_t\sigma_n^2}\right). \tag{22}$$

□

Since the $\lambda(t_h, x, t_t)$ in (22) depends solely on t_t and x, we let

$$\lambda(x, t_t) = \frac{\lambda(t_h, x, t_t)}{(1-p_a)\left(1-p_f\right)B}. \tag{23}$$

Then, we simplify (22) by (23) as

$$\lambda(x, t_t) = xt_t \log\left(1 + \frac{((1-t_t-xt_s)P_h - xe_s)h}{t_t\sigma_n^2}\right). \tag{24}$$

In (24), the sensing time of one subchannel t_s, the energy consumption for sensing each subchannel e_s, the EH power P_h, the channel gain from the ST to the SR h, and the noise variance σ_n^2 are independent of t_t and x. Then, the first-order derivative of $\lambda(x, t_t)$ with respect to x is given by

$$\frac{\partial\lambda(x, t_t)}{\partial x} = t_t \log\left(1 + \frac{((1-t_t-xt_s)P_h - xe_s)h}{t_t\sigma_n^2}\right) - \frac{(t_sP_h + e_s)xht_t}{t_t\sigma_n^2 + (1-t_t-xt_s)P_hh - xe_sh}. \tag{25}$$

Similarly, the first-order derivative of $\lambda(x, t_t)$ with respect to t_t is given by

$$\frac{\partial\lambda(x, t_t)}{\partial t_t} = x \log\left(1 + \frac{((1-t_t-xt_s)P_h - xe_s)h}{t_t\sigma_n^2}\right) + \frac{(xe_s - P_h(1-xt_s))xh}{t_t\sigma_n^2 + (1-t_t-xt_s)P_hh - xe_sh}. \tag{26}$$

The first-order derivative of $\partial\lambda(x, t_t)/\partial x$ in (25) with respect to t_t is given by

$$\frac{\partial^2\lambda(x, t_t)}{\partial x\partial t_t} = \log\left(1 + \frac{((1-t_t-xt_s)P_h - xe_s)h}{t_t\sigma_n^2}\right) - \frac{(P_h(1-xt_s) - xe_s)h\left(t_t\sigma_n^2 + (1-t_t)P_hh\right)}{\left(t_t\sigma_n^2 + (1-t_t-xt_s)P_hh - xe_sh\right)^2}. \tag{27}$$

The second-order derivative of $\lambda(x, t_t)$ with respect to x is given by

$$\frac{\partial^2\lambda(x, t_t)}{\partial x^2} = \frac{-(t_sP_h + e_s)ht_t}{t_t\sigma_n^2 + (1-t_t-xt_s)P_hh - xe_sh} - \frac{(t_sP_h + e_s)ht_t\left(t_t\sigma_n^2 + (1-t_t)P_hh\right)}{\left(t_t\sigma_n^2 + (1-t_t-xt_s)P_hh - xe_sh\right)^2}. \tag{28}$$

The second-order derivative of $\lambda(x, t_t)$ with respect to t_t is given by

$$\frac{\partial^2\lambda(x, t_t)}{\partial t_t^2} = \frac{-x(P_h(1-xt_s)h - xe_sh)^2}{t_t\left(t_t\sigma_n^2 + (1-t_t-xt_s)P_hh - xe_sh\right)^2}. \tag{29}$$

(26) and (27) indicate that $\lambda(x, t_t)$ is a concave function

of x and t_t. Since mixed partial derivatives of $\lambda(x, t_t)$ are continuous for x and t_t, we have

$$\frac{\partial^2 \lambda(x, t_t)}{\partial x \partial t_t} = \frac{\partial^2 \lambda(x, t_t)}{\partial t_t \partial x}. \tag{30}$$

The optimal values of x and t_t, if they ever exist, should satisfy

$$\frac{\partial \lambda(x, t_t)}{\partial x} = 0, \tag{31}$$

$$\frac{\partial \lambda(x, t_t)}{\partial t_t} = 0. \tag{32}$$

Based on (25)-(32), when (31) and (32) hold, we have

$$\begin{aligned} \log\left(1 + \frac{((1 - t_t - xt_s)P_h - xe_s)h}{t_t\sigma_n^2}\right) &= \frac{(t_sP_h + e_s)hx}{t_t\sigma_n^2 + (1 - t_t - xt_s)P_hh - xe_sh} \\ &= \frac{(P_h(1 - xt_s) - xe_s)h}{t_t\sigma_n^2 + (1 - t_t - xt_s)P_hh - xe_sh}, \end{aligned} \tag{33}$$

$$x^* = \frac{P_h}{2t_sP_h + 2e_s}. \tag{34}$$

By bringing the value of x^* in (34) into (33), the optimal solution to t_t, denoted by t_t^* could be obtained. Since (31) and (32) are transcendental equations of t_t, the closed-form solution to t_t could not be obtained. Then, we have

$$\begin{aligned} &\frac{\partial^2 \lambda(x, t_t)}{\partial x^2}\frac{\partial^2 \lambda(x, t_t)}{\partial t_t^2} - \left(\frac{\partial^2 \lambda(x, t_t)}{\partial x \partial t_t}\right)^2 \\ &= -\frac{(P_h(1 - xt_s)h - xe_sh)^2}{(t_t\sigma_n^2 + (1 - t_t - xt_s)P_hh - xe_sh)^2} \\ &\quad - \log^2\left(1 + \frac{((1 - t_t - xt_s)P_h - xe_s)h}{t_t\sigma_n^2}\right) \\ &\quad + 2\log\left(1 + \frac{((1 - t_t - xt_s)P_h - xe_s)h}{t_t\sigma_n^2}\right) \\ &\quad \times \frac{(P_h(1 - xt_s) - xe_s)h\left(t_t\sigma_n^2 + (1 - t_t)P_hh\right)}{(t_t\sigma_n^2 + (1 - t_t - xt_s)P_hh - xe_sh)^2}. \end{aligned} \tag{35}$$

When $x = x^*$ and $t_t = t_t^*$ in (31)-(34) hold, we simplify (35) as

$$\begin{aligned} &\frac{\partial^2 \lambda(x, t_t)}{\partial x^2}\frac{\partial^2 \lambda(x, t_t)}{\partial t_t^2} - \left(\frac{\partial^2 \lambda(x, t_t)}{\partial x \partial t_t}\right)^2\Bigg|_{x=x^*, t_t=t_t^*} \\ &= \frac{2((t_sP_h + e_s)x^*h)^3}{(t_t^*\sigma_n^2 + (1 - t_t^* - x^*t_s)P_hh - x^*e_sh)^3} > 0. \end{aligned} \tag{36}$$

The denominator on the left hand side of the inequality in (36) is positive due to the energy constraint. Namely, the amount of the energy consumed for spectrum sensing x^*e_s should not exceed the amount of the harvested energy $(1 - t_t^* - x^*t_s)P_h$. In addition, we also have

$$\frac{\partial^2 \lambda(x, t_t)}{\partial x^2}\Bigg|_{x=x^*, t_t=t_t^*} < 0, \tag{37}$$

$$\frac{\partial^2 \lambda(x, t_t)}{\partial t_t^2}\Bigg|_{x=x^*, t_t=t_t^*} < 0. \tag{38}$$

Based on (36)-(38) and the second sufficient condition of extreme [33], (x^*, t_t^*) is the optimal solution for $\lambda(x, t_t)$. x^* in (34) and t_t^* in (33) are within the value intervals of $C2 - C3$ in (19) and (20), thus, x^* and t_t^* are feasible. By substituting (x^*, t_t^*) into (23), the maximal $\lambda(x, t_t)$ can be obtained.

However, as pointed out by the proof in Section 3.3, an upper bound of x should be satisfied with respect to the collision constraint. Only with exact values of $p_{d,k}$, P_h, t_s, and e_s, we determine whether the value of x^* in (34) satisfies the collision constraint. Thus, it is essential to present the throughput analysis in the EH-CRN with given duration of the EH phase/sensing phase/transmission phase, respectively, as follows.

5. Throughput Analysis with Given Duration of Each Phase

In this section, we consider three cases of the EH-CRNs: the EH-CRN with given duration of EH phase, the EH-CRN with given duration of sensing phase, and the EH-CRN with given duration of transmission phase. In each case, we formulate and analyze the secondary throughout in various forms, in order to satisfy the upper bound of x provided by the collision constraint in Lemma 2, and other potential requirements about the duration of each phase.

5.1. Given Duration of EH Phase. In this subsection, the duration of EH phase t_h is considered as a constant for the analysis of the expected secondary throughput. We start our analysis based on (9) and (21) as

$$\begin{aligned} \lambda_h(x) &= \frac{\lambda(t_h, x, t_t)}{(1 - p_a)\left(1 - p_f\right)B} \\ &= x(1 - t_h - xt_s)\log\left(1 + \frac{(t_hP_h - xe_s)h}{\sigma_n^2(1 - t_h - xt_s)1 - t_h - xt_s)}\right), \end{aligned} \tag{39}$$

where t_h, t_s, B, p_a, p_f, P_h, e_s, h, and σ_n^2 are viewed as constants. $\lambda_h(x)$ in (39) is a function of the number of sensed subchannels x. The first-order derivative of $\lambda_h(x)$ with respect to x is given by

$$\frac{d\lambda_h(x)}{dx} = (1 - t_h - 2xt_s)\log\left(1 + \frac{(t_hP_h - xe_s)h}{\sigma_n^2(1 - t_h - xt_s)}\right) + \frac{xh\sigma_n^2(t_hP_ht_s - e_s(1 - t_h))}{\sigma_n^2(1 - t_h - xt_s) + (t_hP_h - xe_s)h}. \tag{40}$$

We analyze the numerator of the second item on the right hand side of (40) as

$$xh\sigma_n^2(t_hP_ht_s - e_s(1 - t_h)) < 0 \Rightarrow \frac{t_hP_h}{1 - t_h} - \frac{e_s}{t_s} < 0. \tag{41}$$

Based on the definitions of t_h and P_h in Section 2.1, we infer that $t_hP_h/1 - t_h$ represents the ratio of total harvested energy over the sum of the duration of sensing phase and that of transmission phase. Namely, $t_hP_h/1 - t_h$ represents the average power that the ST consumes energy during the sensing and transmission phase. Based on the definitions of e_s and t_s in Section 2.2, we infer that e_s/t_s represents the average power that the ST consumes energy during the sensing phase. Therefore, (41) represents the case that the average power that the ST consumes energy during the transmission phase is smaller than that during the sensing phase, which is a general scenario as [34]. With respect to (21) and (40), we have

$$\left.\frac{d\lambda_h(x)}{dx}\right|_{x \longrightarrow 0^+} > 0, \tag{42}$$

where $x \longrightarrow 0^+$ represents that x approaches zero from the right. Similarly, we have

$$\left.\frac{d\lambda_h(x)}{dx}\right|_{x \longrightarrow (1 - t_h/t_s)^-} < 0, \tag{43}$$

where $x \longrightarrow (1 - t_h/t_s)^-$ represents that x approaches $1 - t_h/t_s$ from the left. Since $d\lambda_h(x)/dx$ is a continuous function of x, there exists a value of x that satisfies

$$\frac{d\lambda_h(x)}{dx} = 0, \tag{44}$$

where $d\lambda_h(x)/dx$ in (40) is a transcendental equation of x, and the closed-form solution of the x in (44) could not be obtained.

5.2. Given Duration of Sensing Phase. In this subsection, the duration of sensing phase xt_s is considered as a constant. Namely, the number of sensed subchannels x is viewed as a constant. We start our analysis based on (9) and (21) as

$$\lambda_s(t_t) = \frac{\lambda(t_h, x, t_t)}{x(1 - p_a)\left(1 - p_f\right)B} = t_t\log\left(1 + \frac{((1 - t_t - xt_s)P_h - xe_s)h}{\sigma_n^2 t_t}\right), \tag{45}$$

where x, t_s, B, p_a, p_f, P_h, e_s, h, and σ_n^2 are viewed as constants. $\lambda_s(t_t)$ in (43) is a function of the duration of the transmission phase t_t. We use two symbols to simplify (45) as

$$A = 1 - \frac{P_hh}{\sigma_n^2}, \tag{46}$$

$$B = \frac{((1 - xt_s)P_h - xe_s)h}{\sigma_n^2}. \tag{47}$$

We use (46) and (47) in (45) as

$$\lambda_s(t_t) = t_t\log\left(\frac{At_t + B}{t_t}\right), \tag{48}$$

The first-order derivative of $\lambda_s(t_t)$ with respect to t_t is

$$\frac{d\lambda_s(t_t)}{dt_t} = \log\left(\frac{At_t + B}{t_t}\right) - \frac{B}{At_t + B}. \tag{49}$$

As the first-order derivative of $\lambda_s(t_t)$ with respect to t_t is continuous, the second-order derivative of $\lambda_s(t_t)$ with respect to t_t is

$$\frac{d^2\lambda_s(t_t)}{dt_t^2} = -\frac{B^2}{t_t(At_t + B)^2} < 0. \tag{50}$$

With respect to (21) and (49), we have

$$\left.\frac{d\lambda_s(t_t)}{dt_t}\right|_{t_t \longrightarrow 0^+} > 0, \tag{51}$$

$$\left.\frac{d\lambda_s(t_t)}{dt_t}\right|_{t_t \longrightarrow (1 - xt_s)^+} < 0. \tag{52}$$

Based on (48)-(52), we conclude that there exists an optimal value of t_t that maximizes the secondary throughput $\lambda(t_h, x, t_t)$ with given duration of the sensing phase. Since $d\lambda_s(t_t)/dt_t$ in (49) is a transcendental equation of t_t, the closed-form solution of t_t could not be obtained.

5.3. Given Duration of Transmission Phase. In this subsection, the duration of transmission phase t_t is considered as a constant. We start our analysis based on (9) and (21) as

$$\lambda_t(x) = \frac{\lambda(t_h, x, t_t)}{(1 - p_a)\left(1 - p_f\right)Bt_t} = x\log\left(1 + \frac{((1 - t_t - xt_s)P_h - xe_s)h}{\sigma_n^2 t_t}\right), \tag{53}$$

where t_t, t_s, B, p_a, p_f, P_h, e_s, h, and σ_n^2 are viewed as constants. $\lambda_t(x)$ in (53) is a function of the number of sensed subchannels x. We also use two symbols to simplify (53) as follows.

$$C = 1 + \frac{(1 - t_t)P_hh}{\sigma_n^2 t_t}, \tag{54}$$

$$D = \frac{(t_sP_h + e_s)h}{\sigma_n^2 t_t}. \tag{55}$$

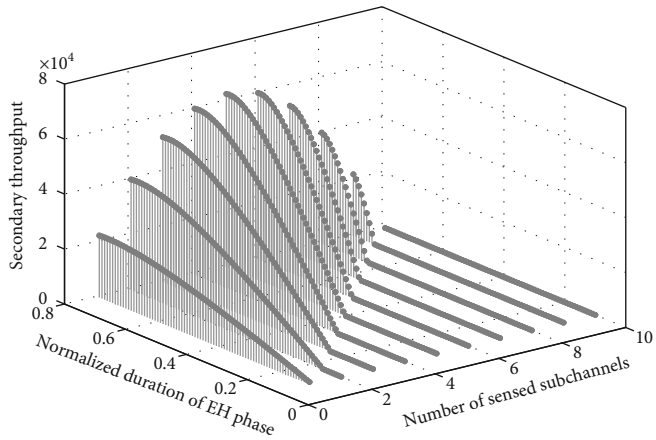

FIGURE 2: The secondary throughput of the EH-CRN with $P_h = 2.5$ mW and $e_s = 0.2$ mJ.

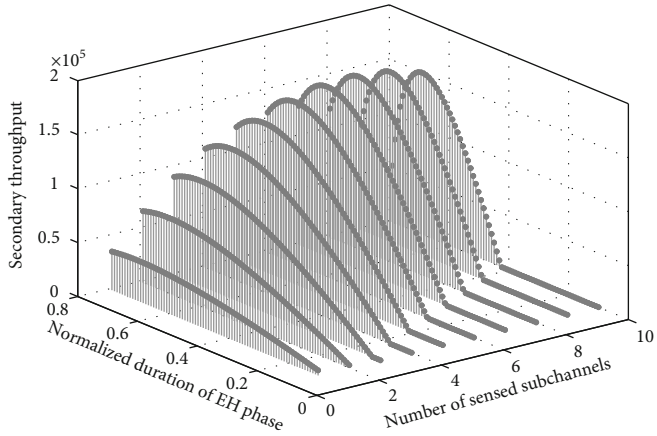

FIGURE 3: The secondary throughput of the EH-CRN with $P_h = 4.7$ mW and $e_s = 0.2$ mJ.

We use (54) and (55) in (53) as

$$\lambda_t(x) = x \log (C - Dx). \tag{56}$$

The first-order derivative of $\lambda_t(x)$ with respect to x is

$$\frac{d\lambda_t(x)}{dx} = \log (C - Dx) - \frac{Dx}{C - Dx}. \tag{57}$$

As the first-order derivative of $\lambda_t(x)$ with respect to x is continuous, the second-order derivative of $\lambda_t(x)$ with respect to x is

$$\frac{d^2\lambda_t(x)}{dx^2} = -\frac{D}{C - Dx} - \frac{CD}{(C - Dx)^2}. \tag{58}$$

Based on definitions of the power, energy, and time parameters, we deduce $C > 0$ and $D > 0$. Then, we deduce that the second-order derivative of $\lambda_t(x)$ with respect to x is negative. With respect to (21) and (57), we have

$$\left.\frac{d\lambda_t(x)}{dx}\right|_{x \longrightarrow 0^+} > 0, \tag{59}$$

$$\left.\frac{d\lambda_t(x)}{dx}\right|_{x \longrightarrow (1 - t_t/t_s)^-} < 0. \tag{60}$$

Based on (57)-(60), we conclude that there exists an optimal value of x that maximizes the secondary throughput $\lambda(t_h, x, t_t)$ with given duration of the transmission phase. Since $d\lambda_t(x)/dx$ in (55) is a transcendental equation of x, the closed-form solution of x could not be obtained.

6. Numerical Results

In this section, we provide numerical results to validate the theoretical results about the secondary throughput $\lambda(t_h, x, t_t)$ in the EH-CRN. We introduce the values of network parameters as follows. Without loss of generality, the length of a time slot is normalized. The probability that each subchannel is active $p_a = 0.8$, the sensing time of one subchannel $t_s = 0.02$, the probability of false alarm $p_f = 0.1$, the bandwidth of each channel $B = 10^6$ Hz, the gain of the channel from the ST to the SR $h = -40$dB, and the noise power for the secondary packet transmission $\sigma_n^2 = -50$ dBm.

From the perspective of energy, we consider the amount of the energy consumed for sensing one subchannel $e_s = 0.2$

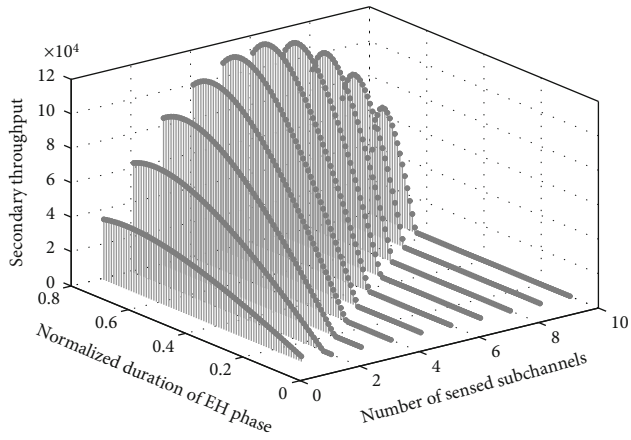

FIGURE 4: The secondary throughput of the EH-CRN with $P_h = 4.7$ mW and $e_s = 0.3$ mJ.

mJ, and the EH power of the ST $P_h = 2.5$ mW unless otherwise specified. The values of network parameters are set according to those in [34, 35].

Figure 2 plots the secondary throughput of the EH-CRN $\lambda(t_h, x, t_t)$ of the EH-CRN with $P_h = 2.5$ mW and $e_s = 0.2$ mJ. Then, we have observations listed as follows: (1) when the normalized duration of EH phase t_h is relative short and the number of sensed channels x is relatively large, the secondary throughput is zero. (2) $\lambda(t_h, x, t_t)$ first increases with x and then decreases with x, which indicates that the optimal number of sensed channels $x^* = 5$. (3) $\lambda(t_h, x, t_t)$ first increases with t_h and then decreases with x. The reason for observation (1) is that the energy harvested by the ST is no larger than the energy consumption of spectrum sensing, and the ST does not have available energy for packet transmission. The observation (2) is in accordance with the theoretical result in (34). By bringing the values of P_h, t_s, and e_s into (34), we obtain $x^* = 5$, which validates the correctness of x^* in (34). Observation (3) validates the existence of the optimal t_h, and the correctness of t_h^* in (32). Besides, observation (3) is in accordance with the theoretical results in Sections 5.2 and 5.3.

Figure 3 plots the secondary throughput of the EH-CRN $\lambda(t_h, x, t_t)$ of the EH-CRN with $P_h = 4.7$ mW and $e_s = 0.2$ mJ. Observations (1) and (3) from Figure 2 also hold for Figure 3. By bringing the values of P_h, t_s, and e_s into (34), we obtain $x^* = 8$, which is in accordance with the observation from Figure 3. Therefore, the optimal number of sensed channels x^* only depends on the EH power of the ST P_h, the sensing time of one subchannel t_s, and the amount of the energy consumed for sensing one subchannel e_s. Besides, by comparing Figures 2 and 3, the maximum secondary throughput increases with the EH power of the ST, which is due to the reason that more energy supply could be exploited by the ST for secondary packet transmission.

Figure 4 plots the secondary throughput of the EH-CRN $\lambda(t_h, x, t_t)$ of the EH-CRN with $P_h = 4.7$ mW and $e_s = 0.3$ mJ. By bringing the values of P_h, t_s, and e_s into (34), we obtain $x^* = 6$, which is in accordance with the observation from Figure 4. Therefore, the optimal number of sensed channels x^* decreases with the energy consumption of sensing one subchannel e_s, and the maximum secondary throughput decreases with e_s. This observation is due to the reason that, with the increase of e_s, the ST has less energy for packet transmission and has to reduce the number of sensed channels to lower the energy consumption, in order to satisfy the energy constraint in the throughput optimization problem.

7. Conclusions

In this paper, we have studied the throughput and collision performances of the multichannel EH-CRNs consisting of M primary pairs and one secondary pair. To tackle the time tradeoff among EH, sequential sensing, and packet transmission in the time slot where the number of sensed channels is considered as a variable, we formulate the secondary throughput with respect to the durations of the three phases and prove the existence of the optimal time allocation through monotonicity analysis. Numerical results validate the theoretical results about the secondary throughput. We find that the optimal number of sensed channels during the sensing phase only depends on the EH power of the ST, the sensing time of one subchannel, and the energy consumed for sensing one subchannel.

Data Availability

No data were used to support this study.

Conflicts of Interest

All authors declared that they do not have any conflicts of interest.

Acknowledgments

This work is supported in part by the National Nature Science Foundation of China, Grant numbers: 61902351, 61902353, and 61802346; Zhejiang Provincial Natural Science Foundation of China, Grant numbers: LY21F020022, LY21F020023, and LQ22F020009; Zhejiang Provincial Research Project on the Application of Public Welfare Technologies, Grant number: LGF22F020023.

References

[1] L. Liu, M. Zhao, M. Yu, M. A. Jan, D. Lan, and A. Taherkordi, "Mobility-aware multi-hop task offloading for autonomous driving in vehicular edge computing and networks," *IEEE Transactions on Intelligent Transportation Systems*, pp. 1–14, 2022.

[2] Y. Xu, J. Liu, Y. Shen, J. Liu, X. Jiang, and T. Taleb, "Incentive jamming-based secure routing in decentralized internet of things," *IEEE Internet of Things Journal*, vol. 8, no. 4, pp. 3000–3013, 2021.

[3] J. Liu, Y. Xu, Y. Shen, H. Takakura, X. Jiang, and T. Taleb, "Buffer space management in intermittently connected internet of things: sharing or allocation?," *IEEE Internet of Things Journal*, vol. 9, no. 13, pp. 10961–10977, 2022.

[4] J. Feng, L. Liu, Q. Pei, and K. Li, "Min-max cost optimization for efficient hierarchical federated learning in wireless edge

networks," *IEEE Transactions on Parallel and Distributed Systems*, vol. 33, no. 11, pp. 2687–2700, 2022.

[5] L. Liu, J. Feng, Q. Pei et al., "Blockchain-enabled secure data sharing scheme in mobile-edge computing: an asynchronous advantage actor-critic learning approach," *IEEE Internet of Things Journal*, vol. 8, no. 4, pp. 2342–2353, 2021.

[6] H. Han, L. Fang, W. Lu, W. Zhai, Y. Li, and J. Zhao, "A GCICA grant-free random access scheme for M2M communications in crowded massive MIMO systems," *IEEE Internet of Things Journal*, vol. 9, no. 8, pp. 6032–6046, 2022.

[7] X. Liu, K. Zheng, K. Chi, and Y. Zhu, "Cooperative spectrum sensing optimization in energy-harvesting cognitive radio networks," *IEEE Transactions on Wireless Communications*, vol. 19, no. 11, pp. 7663–7676, 2020.

[8] X. Liu, K. Zheng, L. Fu, X. Y. Liu, X. Wang, and G. Dai, "Energy efficiency of secure cognitive radio networks with cooperative spectrum sharing," *IEEE Transactions on Mobile Computing*, vol. 18, no. 2, pp. 305–318, 2019.

[9] K. Zheng, X. Liu, Y. Zhu, K. Chi, and K. Liu, "Total throughput maximization of cooperative cognitive radio networks with energy harvesting," *IEEE Transactions on Wireless Communications*, vol. 19, no. 1, pp. 533–546, 2020.

[10] P. Ramezani and A. Jamalipour, "Toward the evolution of wireless powered communication networks for the future internet of things," *IEEE Network*, vol. 31, no. 6, pp. 62–69, 2017.

[11] K. Zheng, X.-Y. Liu, X. Liu, and Y. Zhu, "Hybrid overlay-underlay cognitive radio networks with energy harvesting," *IEEE Transactions on Communications*, vol. 67, no. 7, pp. 4669–4682, 2019.

[12] A. Gharib, W. Ejaz, and M. Ibnkahla, "Enhanced multiband multiuser cooperative spectrum sensing for distributed CRNs," *IEEE Transactions on Cognitive Communications and Networking*, vol. 6, no. 1, pp. 256–270, 2020.

[13] S.-J. Kim and G. B. Giannakis, "Sequential and cooperative sensing for multi-channel cognitive radios," *IEEE Transactions on Signal Processing*, vol. 58, no. 8, pp. 4239–4253, 2010.

[14] S. Kang, C. Joo, J. Lee, and N. B. Shroff, "Pricing for past channel state information in multi-channel cognitive radio networks," *IEEE Transactions on Mobile Computing*, vol. 17, no. 4, pp. 859–870, 2018.

[15] W. Cheng, W. Zhang, L. Liang, and H. Zhang, "Full-duplex for multi-channel cognitive radio ad hoc networks," *IEEE Network*, vol. 33, no. 2, pp. 118–124, 2019.

[16] Y. Li, W. Zhang, C.-X. Wang, J. Sun, and Y. Liu, "Deep reinforcement learning for dynamic spectrum sensing and aggregation in multi-channel wireless networks," *IEEE Transactions on Cognitive Communications and Networking*, vol. 6, no. 2, pp. 464–475, 2020.

[17] A. Celik and A. E. Kamal, "Multi-objective clustering optimization for multi-channel cooperative spectrum sensing in heterogeneous green CRNs," *IEEE Transactions on Cognitive Communications and Networking*, vol. 2, no. 2, pp. 150–161, 2016.

[18] W. Ejaz and M. Ibnkahla, "Multiband spectrum sensing and resource allocation for IoT in cognitive 5G networks," *IEEE Internet of Things Journal*, vol. 5, no. 1, pp. 150–163, 2018.

[19] A. Alsharoa, N. M. Neihart, S. W. Kim, and A. E. Kamal, *Multi-Band RF Energy and Spectrum Harvesting in Cognitive Radio Networks*, Proc. IEEE ICC, Kansas City, MO, USA, 2018.

[20] P. D. Thanh, T. N. K. Hoan, and I. Koo, "Joint resource allocation and transmission mode selection using a POMDP-based hybrid half-duplex/full-duplex scheme for secrecy rate maximization in multi-channel cognitive radio networks," *IEEE Sensors Journal*, vol. 20, no. 7, pp. 3930–3945, 2020.

[21] A. Bagheri and A. Ebrahimzadeh, "Statistical analysis of lifetime in wireless cognitive sensor network for multi-channel cooperative spectrum sensing," *IEEE Sensors Journal*, vol. 21, no. 2, pp. 2412–2421, 2021.

[22] K. Cichon, A. Kliks, and H. Bogucka, "Energy-efficient cooperative spectrum sensing: a survey," *IEEE Communication Surveys and Tutorials*, vol. 18, no. 3, pp. 1861–1886, 2016.

[23] W. Sun, X. Liu, K. Zheng, Y. Xu, and J. Liu, *Spectrum Utilization Improvement for Multi-Channel Cognitive Radio Networks with Energy Harvesting*, International Conference on Networking and Network Applications (NaNA), Guilin, China, 2021.

[24] C. Jiang, Y. Chen, K. J. R. Liu, and Y. Ren, "Renewal-theoretical dynamic spectrum access in cognitive radio network with unknown primary behavior," *IEEE Journal on Selected Areas in Communications*, vol. 31, no. 3, pp. 406–416, 2013.

[25] A. Ali and W. Hamouda, "Advances on spectrum sensing for cognitive radio networks: theory and applications," *IEEE Communication Surveys and Tutorials*, vol. 19, no. 2, pp. 1277–1304, 2017.

[26] E. Axell, G. Leus, E. G. Larsson, and H. V. Poor, "Spectrum sensing for cognitive radio : state-of-the-art and recent advances," *IEEE Signal Processing Magazine*, vol. 29, no. 3, pp. 101–116, 2012.

[27] Y.-C. Liang, Y. Zeng, E. Peh, and A. T. Hoang, "Sensing-throughput tradeoff for cognitive radio networks," *IEEE Transactions on Wireless Communications*, vol. 7, no. 4, pp. 1326–1337, 2008.

[28] M. Laghate and D. Cabric, "Cooperative spectrum sensing in the presence of correlated and malicious cognitive radios," *IEEE Transactions on Communications*, vol. 63, no. 12, pp. 4666–4681, 2015.

[29] A. Celik, A. Alsharoa, and A. E. Kamal, "Hybrid energy harvesting-based cooperative spectrum sensing and access in heterogeneous cognitive radio networks," *IEEE Transactions on Cognitive Communications and Networking*, vol. 3, no. 1, pp. 37–48, 2017.

[30] S. Yin, Z. Qu, and S. Li, "Achievable throughput optimization in energy harvesting cognitive radio systems," *IEEE Journal on Selected Areas in Communications*, vol. 33, no. 3, pp. 407–422, 2015.

[31] S. H. A. Ahmad, M. Liu, T. Javidi, Q. Zhao, and B. Krishnamachari, "Optimality of myopic sensing in multi-channel opportunistic access," *IEEE Transactions on Information Theory*, vol. 55, no. 9, pp. 4040–4050, 2009.

[32] C. E. Shannon, "A mathematical theory of communication," *The Bell System Technical Journal*, vol. 27, no. 3, pp. 379–423, 1948.

[33] A. D. Polyanin and A. V. Manzhrov, *Handbook of Mathematics for Engineers and Scientists*, Chapman & Hall/CRC Press, LCC, New York, USA, first edition edition, 2007.

[34] S. Park, H. Kim, and D. Hong, "Cognitive radio networks with energy harvesting," *IEEE Transactions on Wireless Communications*, vol. 12, no. 3, pp. 1386–1397, 2013.

[35] K. Zheng, X. Liu, B. Wang, H. Zheng, K. Chi, and Y. Yao, "Throughput maximization of wireless-powered communication networks: an energy threshold approach," *IEEE Transactions on Vehicular Technology*, vol. 70, no. 2, pp. 1292–1306, 2021.